The 4th European sCO_2 Conference for Energy Systems
March 23-24, 2021, Online Conference

2021-sCO2.eu-135

NUMERICAL DIMENSIONING OF A PRE-COOLER FOR SCO_2 POWER CYCLES TO UTILIZE INDUSTRIAL WASTE HEAT

Sebastian Unger*
HZDR, Institute of Fluid Dynamics
Dresden, Germany
Email: s.unger@hzdr.de

Jonas Müller
HZDR, Institute of Fluid Dynamics
Dresden, Germany

Malini Bangalore Mohankumar
HZDR, Institute of Fluid Dynamics
Dresden, Germany

Sebastian Rath
Technical University Dresden,
Institute of Power Engineering,
Dresden, Germany

Uwe Hampel
HZDR, Institute of Fluid Dynamics
Dresden, Germany

ABSTRACT

The annual waste heat available from industry in the European Union is more than 2,700 PJ. Consequently, the utilization of the unexploited thermal energy will decisively contribute to a reduced overall power consumption and lower greenhouse gas emissions. Supercritical carbon dioxide (sCO_2) power cycles offer a variety of advantages for that purpose compared to established power cycles. Such are a high conversion efficiency and a turbomachinery with high power density. The pre-cooler is one of the essential components in an sCO_2 power cycle and the prediction of the flow and heat transfer characteristics is a challenging task. In the present investigation, cycle layouts were developed for one waste heat source: a gas compressor station. The pre-cooler design as well as the boundary conditions of the numerical simulation were assessed by an analytical model. The most promising design was the printed circuit heat exchanger with inlet temperatures between 209 °C and 352 °C. Subsequently, these heat exchangers were examined in more detail by the numerical code ANSYS CFX for sCO_2 mass fluxes between 100 kg/(m² s) and 900 kg/(m² s). The pressure drop along the sCO_2 channel was found insensitive to the channel diameter, but increased with the channel length and mass flux. However, the pressure drop of the coolant stream significantly depends on the channel diameter and thus a larger coolant channel diameter is recommended to maintain a reasonably low pressure drop. The overall heat transfer coefficient is limited by the heat transfer on the coolant side. Ultimately, pre-cooler designs were proposed for a waste heat system of a gas compressor station, consisting of compact modular stainless steel plates with an sCO_2 channel diameter of 0.5 mm, a coolant channel diameter of 0.8 mm, an sCO_2 mass flux of 700 kg/(m² s) and a coolant mass flux of 1029 kg/(m² s). Based on these results more complex channels designs, including internal fins were studied. The fin height was optimized, in order to improve the heat transfer performance.

INTRODUCTION

An enhanced energy utilization is an upcoming requirement in many industrial processes, in order to reduce energy consumption while maintaining economic prosperity [1]. One of the highest energy demands occur in the industrial sector. A considerable amount of the energy consumption is rejected and lost to the environment by waste heat. Thus, the recovery of the waste heat is essential to improve the overall energy utilization, to enhance the efficiency and to reduce the carbon foot print of industrial applications. Therefore, existing technologies for waste heat recovery aim to reconvert the waste heat into mechanical - and furthermore into electrical power. The supercritical CO_2 power cycle represents an attractive alternative to the established power cycles. An essential component in an sCO_2 power cycle is the pre-cooler, which cools the CO_2 close to the critical point in order to achieve optimal compressor inlet conditions required to minimize the compression work. The design of the pre-cooler may be a challenging task due to the complex heat transfer behavior [2].

Thus, Liao and Zhao [3] experimentally investigated the heat transfer of carbon dioxide under cooling conditions in horizontal tubes of 0.5 mm to 2.16 mm diameter. The influences of mass flux, inlet temperature, and pressure were investigated. The results showed a significant influence of buoyancy on the HTC up to Reynolds number of 105. The influence became weaker with decreasing tube diameter and increasing Reynolds number. Dang and Hihara [4] investigated the heat transfer and pressure drop of CO_2 in horizontal tubes with diameter between 1 mm and 6 mm. In the study, the heat transfer coefficient increases with mass flux and reducing tube diameter. Ngo et al.

* corresponding author(s)

DOI: 10.17185/duepublico/73968

[5] performed experiments with zigzag and s-shaped fins on micro-channel heat exchangers. The s-shaped fins showed slightly smaller heat transfer, but significantly less pressured drop compared to the zigzag channel. Li et al. [6] performed experimental investigations on the heat transfer of CO_2 in printed circuit heat exchangers for heating and cooling conditions. The heat transfer coefficient reaches a maximum when the temperature approaches the pseudo-critical point (the pseudo-critical point is defined as the temperature, for a given pressure, at which the specific heat exhibits a maximum). The numerical work of Pitla et al. [7] studied the turbulent heat transfer of sCO_2 under cooling conditions. A validation of the numerical model by experimental data was done. Van Abel et al. [8] applied numerical methods to investigate a PCHE with zigzag channels regarding heat transfer and pressure drop. The zigzag channels achieved great heat transfer compared to the straight channel. Serrano et al. [9] developed mathematical models based on empirical correlations for the heat transfer of printed circuit heat exchangers. Based on these model optimized sizing and performance of heat exchangers for fusion power plants were proposed. Xu et al. [10] studied airfoil-shaped fins in a printed circuit heat exchanger. It was found, that the staggered fin arrangement is more suitable than a parallel fin arrangement. Baik et al. [11] investigated the performance of wavy-channel printed circuit heat exchangers and found a significant enhancement compared to the straight channels. Furthermore, an increase of wave amplitude or decrease of wave period improves the heat exchanger performance. In the numerical model of Wang et al. [12] the turbulent heat transfer of cooled sCO_2 in horizontal tubes was studied. A wide range of different operation condition was analyzed a heat transfer correlations proposed. The heat transfer increases with mass flux, tube diameter and close to the pseudo-critical point. From the literature survey it can be seen, that several studies analyze the heat transfer behavior of sCO_2 under cooling conditions by experimental and numerical methods. Some authors investigate novel channel geometries and flow paths such as airfoil-shape and zigzag channels. The present study aims to propose a pre-cooler for a sCO_2 power cycle, which recovers industrial waste heat. Based on the boundary conditions, determined by the power cycle, the channel diameters for both fluid will be numerical optimized. For the optimum design an internal fin geometry will introduced and studied.

ANALYSIS OF INDUSTRIAL WAST HEAT SOURCES

Industrial waste heat is heat, which arises in industrial processes as an undesired byproduct due to inefficiencies and thermodynamic limitations in the equipment and processes. This chapter aims to give an overview on the recovery of industrial waste heat in the European Union. In the present study the sources will analyzed based on heat quantity and heat quality. In the end of the chapter, two possible industrial waste heat sources will be selected for the subsequent investigation.

The project "Heat Roadmap Europe" aims to analyses the heating and cooling sector in Europe in order to identify potentials for sustainable heating and decarburization [13]. In the study of Connolly et al. [14] this values for the industrial waste heat amounts for 27 individual countries in the European Union were presented. In another study, Persson et al. used the European Pollutant Release and Transfer Register in combination with sector-specific standard efficiencies to determine the waste heat potential [15]. Based on both studies, Figure 1 compares the distribution of the potential waste heat amount of the individual countries.

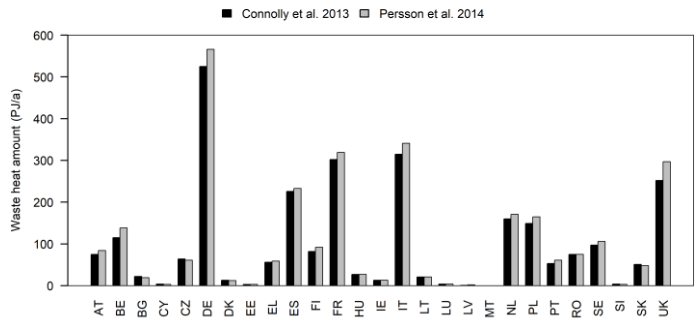

Figure 1: Industrial waste heat amount of individual countries in the European Union according to [14] and [15].

Brückner [16] estimated the lower limitation of waste heat from exhaust gas for Germany from the emission law database. A lower reference temperature of 35 °C was assumed as standardized value to evaluate the waste heat potential. The cumulative industrial waste heat amount of Germany is shown in Figure 2 for different temperature T_{src}, Carnot efficiency η_C and amounts of waste heat $\dot{Q}_{wh}$. The most relevant industry sectors for utilizing waste heat are the cement industry, ceramic industry, iron and steel industry, aluminum and copper industry, glass industry, chemical industry, gas transmission and storage, paper and pulp industry as well as the food industry.

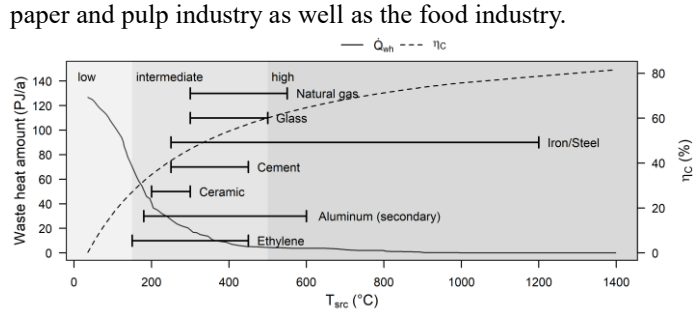

Figure 2: Cumulative industrial waste heat amount $\dot{Q}_{wh}$ of Germany with respect to temperature T_{src} and Carnot efficiency η_C [16].

It is evident that the extraction and transport of natural gas has a considerable waste heat potential. For the present study, a specific industry is selected as an example for waste heat recovery. In this context, the exemplary waste heat utilization of a gas compressor station was selected as a reference for this study. In this case, the main component delivering the mechanical energy for the compression is usually a gas turbine fueled by the natural gas branched from the pipelines with an air-fuel equivalence of λ=5. The waste heat of this turbine remains

unused in many cases and were therefore considered as a heat source for the present investigation. The parameters were oriented at the MAN 1304-12N [17]. Both the turbine and the Parameters are shown in Figure 3. A steady-state operation of the waste heat source was assumed for the subsequent calculations.

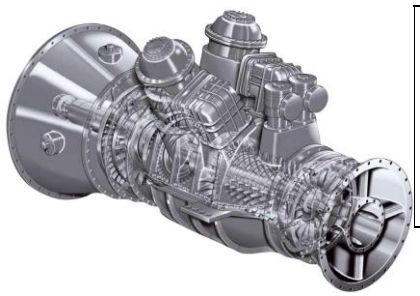

Waste heat stream parameters:
$T_{wh} = 515\ °C$
$\dot{m}_{wh} = 49.1\ kg/s$
$\dot{Q}_{wh} = 28.5\ MW$

Figure 3: Selected waste heat source - MAN 1304-12 gas turbine and the corresponding waste heat stream parameters [17].

POWER CYCLE AND PRE-COOLER SELECTION

There are several sCO_2 power cycle layouts to convert thermal power into mechanical power. A mathematical model of the power cycle was developed in MATLAB and two scenarios were analyzed. As depicted in Figure 4 these are a simple layout including compressor, primary heat exchanger, turbine and pre-cooler, as well as the same layout including a recuperator.

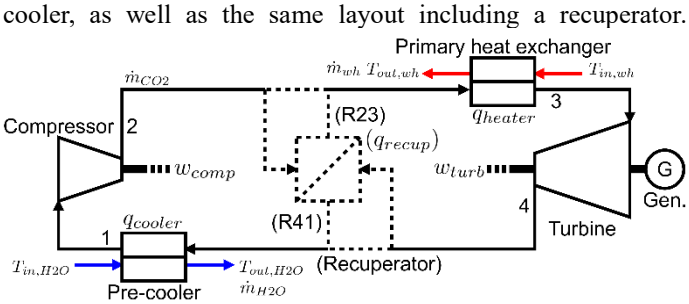

Figure 4: sCO_2 power cycle for waste heat recovery.

Both designs were calculated for a minimum pressure of 75 bar, a minimum temperature of 35 °C, a terminal temperature difference of 5 K and the efficiencies shown in Table 1.

Table 1: Efficiencies of the components in the power cycle.

Component	Turbine	Compressor	Recuperator
Efficiency	90 %	85 %	90 %

As one can see from Figure 5 the net power output of the recuperated cycle is only 5% higher compared to the power cycle without recuperator. Since the heat exchanger inlet temperature is higher in case of a recuperated cycle, the heat flow of the waste heat stream can only be utilized to this lower temperature. As a consequence, waste heat stream temperature leaves the primary heat exchanger at higher temperature and a considerable amount of thermal energy will not been used. In future studies the utilization of the remaining heat will be investigated. Based on this result, a pre-cooler was selected operating at an inlet pressure of 7.5 MPa, a mass flow rate of 85.6 kg/s and temperature up to 352 °C.

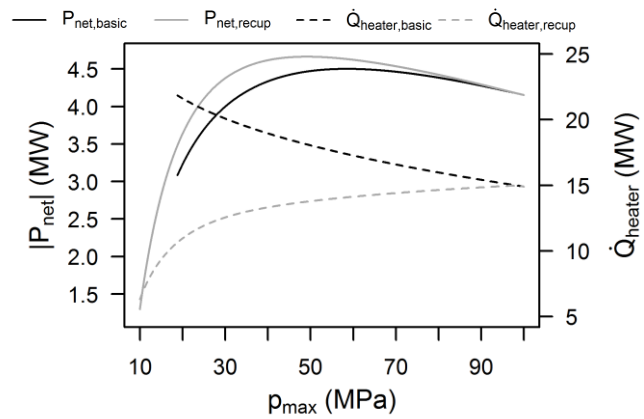

Figure 5: Net power and heat duties of the sCO_2 power cycle.

NUMERICAL MODEL

The commercial fluid dynamic code ANSYS CFX was applied to simulate the pre-cooler. The geometry consists of a sCO_2 channel, a coolant channel and a heat exchanger body. Both channels are divided into an entrance section, a heat exchanger section and an exit section as one can see in Figure 6. The inlet temperature and pressure of the coolant channel was 35 °C and 1 bar. The entrance sections were considered to achieve a fully developed flow in the heat transfer area, in order to have comparable flow conditions. However, in a real application the fluid flows into the individual channels from a header (distributer) and may not be fully developed. The top and bottom part of the solid body uses periodic boundaries, the side of the domains were defined as symmetry and between the channels and the solid body, heat transfer conjugation was used. The solid material was assumed to be 316 L with an thermal conductivity of 16.2 W/mK.

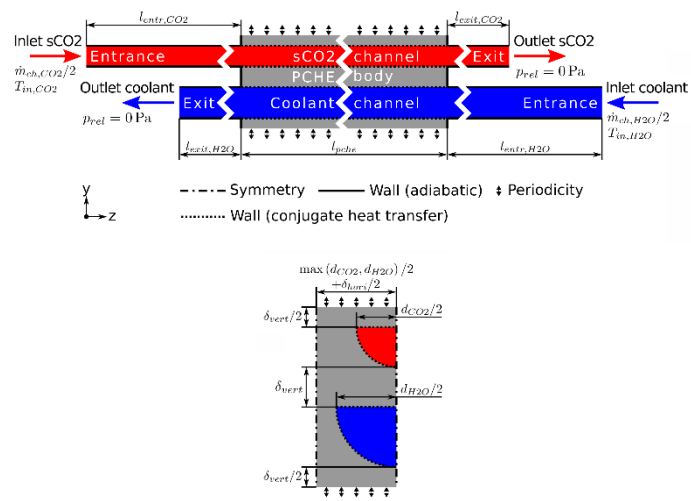

Figure 6: Domains, boundary conditions and geometry of the pre-cooler model.

In this investigation the fluid properties of sCO_2 is taken from the CoolProp library. The used conservation equations for mass, momentum and energy, also known as Navier-Stokes equations are

$$\frac{\rho \delta u_I}{\delta x_I}=0 \quad \textbf{(1)}$$

$$\rho\left(u_J\frac{\delta u_I}{\delta x_J}\right)=-\frac{\delta p}{\delta x_I}+\frac{\delta}{\delta x_J}\left(\left(\mu+\mu_T\right)\left(\frac{\delta u_I}{\delta x_J}+\frac{\delta u_J}{\delta x_I}\right)\right) \quad \textbf{(2)}$$

$$\rho c_p\left(u_J\frac{\delta T}{\delta x_J}\right)=\frac{\delta}{\delta x_J}\left(\left(\lambda+\frac{\mu_T c_p}{Pr_T}\right)\frac{\delta T}{\delta x_J}\right). \quad \textbf{(3)}$$

These partial differential equations are discretized and the velocity vector field and scalar temperature filed were solved numerically. The turbulent Prandtl number has been set to Pr_T=0.9 as suggested by Yuan [18] and the turbulent viscosity μ_T was calculated by

$$\mu_T=\varrho\frac{k}{\omega} \quad \textbf{(4)}$$

The Reynolds number of the coolant channel is approximately at 450 and thus the flow was modeled as laminar. Since the Reynolds number varies between 7,000 and 14,000 for the sCO2 channel in the present study, the Shear Stress Transport (SST) model was applied for the transient and turbulent region, to calculate the turbulence kinetic energy and the turbulence frequency. Furthermore, the experimental results of Kruizenga et al. [19] as well as the pressure drop correlation of Blasius and Colebrook were used to validate the numerical model for two different operating conditions, which is a mass flux of 326 kg/(m²s) and 762 kg/(m²s) for a channel diameter of 1.9 mm. This comparison is shown in Figure 7 for the heat transfer and in Figure 8 for the pressure drop. The heat transfer can be predicted with sufficient accuracy and the pressure drop is very well represented.

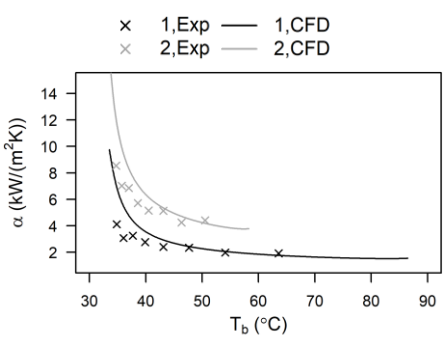

Figure 7: Validation of the heat transfer of the CFD model by experiments from literature.

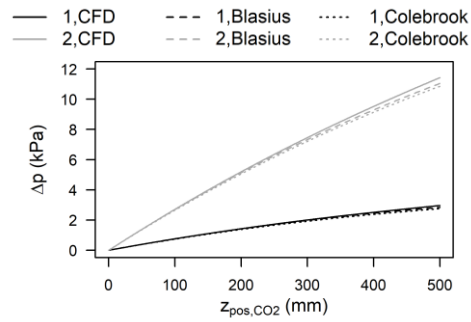

Figure 8: Validation of the pressure drop of the CFD model by empirical correlations from literature.

In order to validate the independency of the numerical results from the applied mesh, eight different meshes of different grid density were studied. A hexaeder dominant grid was applied, using inflation layer on the boundary between fluid and solid and the element size was controlled along the flow channels and at the cross section. In the Figure 9 the heat transfer coefficient and in the Figure 10 the pressure drop are shown along both channels from the finest mesh 1 to the coarsest mesh 8. The mesh 2 having 2.5 million nodes was used for further analysis, since there is no improvement to the mesh 1. Additionally, the boundary layer can be well resolved for a dimensionless wall distance of y+ < 1.

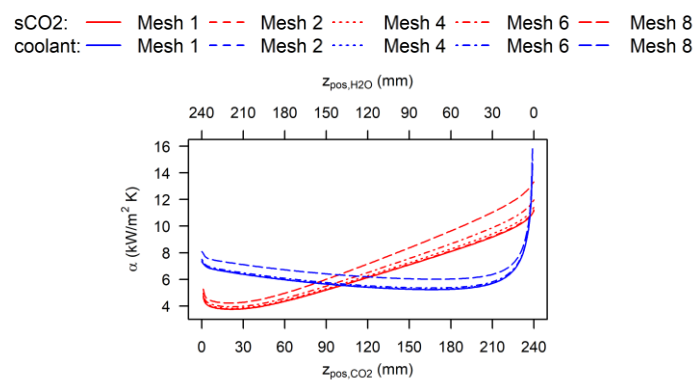

Figure 9: Heat transfer results of the mesh independency study.

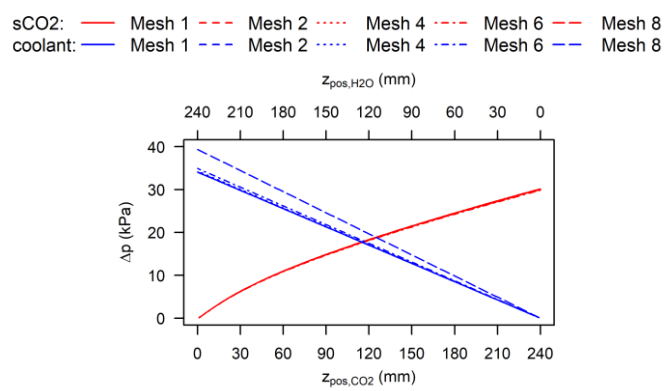

Figure 10: Pressure drop results of the mesh independency study.

The numerical simulation was used to study the effect of channel diameter for both fluids between 0.5 mm and 1.1 mm. For assessment of the pre-cooler, the volumetric heat flux and the pressure drop were used. Here, the volumetric heat flux represents the heat flow per volume of the heat exchanger.

RESULTS OF THE SIMULATION

In the Figure 11 the numerical results are visualized for different axial positions along the sCO_2 channel for a 0.5 mm sCO_2 channel, a 0.8 mm coolant channel and a sCO_2 mass flux density of 700 kg/(m²s). It can be seen, that at the 40 mm position the temperature and velocity distribution are still inhomogeneous, from 80 mm on both distributions become more homogeneous and nearly equalize.

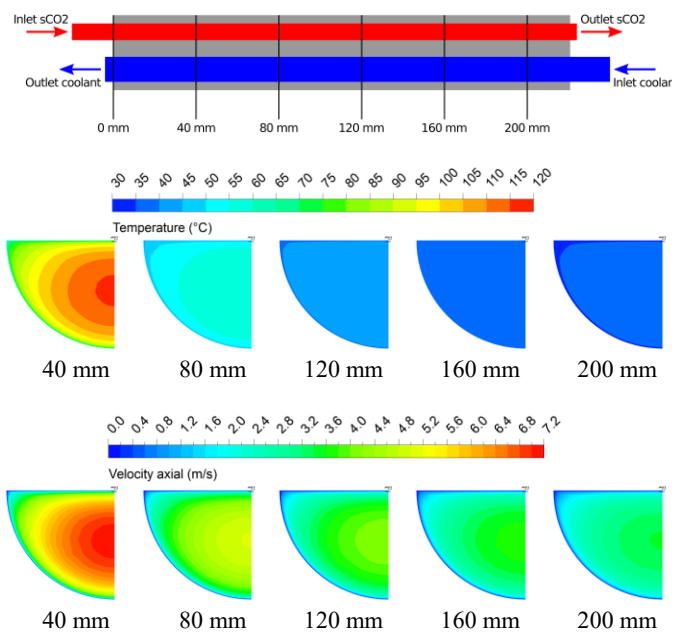

Figure 11: Temperature and velocity distribution of the sCO_2 channel at different axial positions.

The numerical results were compared with empirical results calculated from the Jackson correlation [20] for the heat transfer and the Colebrook correlation for pressure drop. The diameter of the coolant channel was changed from 0.5 mm to 0.8 mm and 1.1 mm, and the diameter of the sCO_2 channel was changed between 0.5 mm and 0.8 mm. The heat transfer results of different combinations of the channel dimensions are shown in Figure 12 and Figure 13 for different mass flux. In this and the following plots, the combination of sCO_2 channel to coolant channel diameter are expressed as sCO_2-coolant, e.g. 5-11 represents a 0.5 mm sCO_2 channel and a 1.1 mm coolant channel diameter. As expected the heat transfer increases with the mass flux, due to higher convection. Furthermore, the smallest channel diameter achieve the greatest heat transfer performance. In case of the 8-5 configuration there is a sharp increase in the analytical, correlation based, calculation. This is due to the change in flow regime from laminar to turbulent within the calculation scheme.

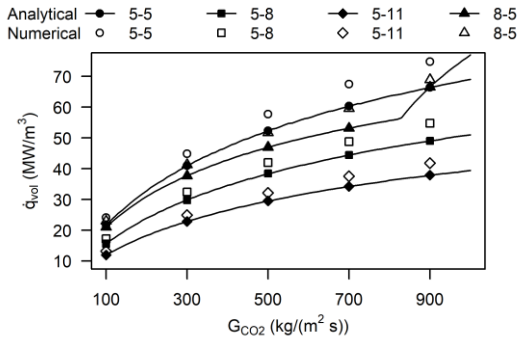

Figure 12: Numerical and analytical heat flux density results for different channel diameter.

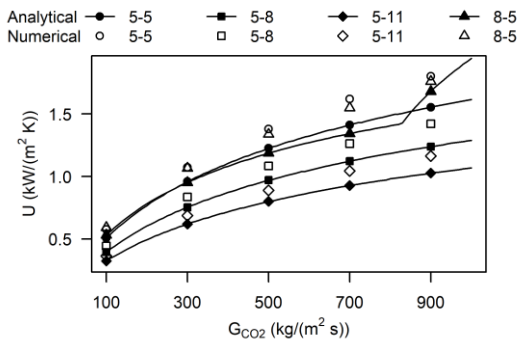

Figure 13: Numerical and analytical overall heat transfer coefficient results for different channel diameter.

The pressure drop characteristics of both channels is shown in Figure 14 for the CO_2 side and in Figure 15 for the coolant side for varying mass fluxes. Similar to the heat transfer increases the pressure drop for both channels as the mass flux rises. The pressure drop of the sCO_2 channel changes only little with geometry. In fact, only the 8-5 configuration increases the pressure loss, due to a decrease of heat transfer surface area and consequently longer channel length. The pressure drop in the coolant channel increases as the channel diameter reduces. In fact, the highest pressure drop occur for the 0.5 mm channel diameter. One reason may be the reduced friction surface area at lower channel diameter. The pressure drop of the 8-5 configuration is very high, since the required mass flux to transfer the heat is higher.

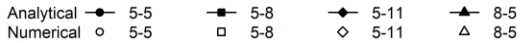

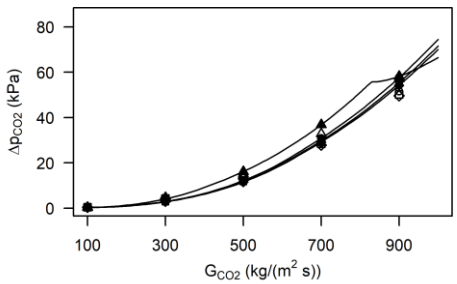

Figure 14: Numerical and analytical pressure drop results of the CO_2 for different channel diameter.

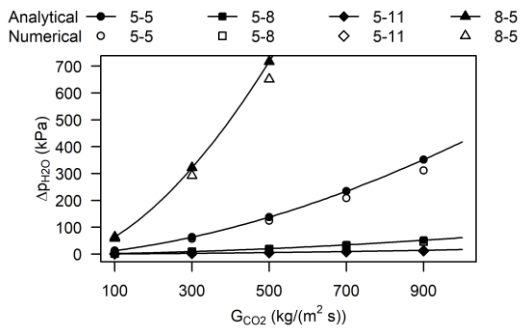

Figure 15: Numerical and analytical pressure drop results of the coolant for different channel diameter.

As one can see, the heat transfer as well as the pressure drop both increase as the channel diameter reduce. In order to determine a beneficial configuration, the global performance of the pre-cooler for the sCO_2 flow path will be calculated. The global performance criterion represents the ratio of heat flow to the required pumping power due to pressure drop and is shown in Figure 16 for the CO_2 side and in Figure 17 for the coolant side. The global performance reduces as the mass flux density increases, due to the strong increase in pressure drop. As the mass flux exceeds 300 kg/(m²s) the global performance criterion is almost independent of the channel diameter for the sCO_2 channel. However, the global performance related to the coolant channel is strongly influenced by the channel diameter. It can be seen, that a higher diameter results in a superior performance. Hence, a high coolant channel dimeter and a small sCO_2 channel diameter was chosen and used for further analysis. In fact, the configuration 5-8 achieves the greatest performance at a mass flux of approximately 700 kg/(m²s). At this parameters a compactness of 627 m²/m³ can be achieved. In general analytical and numerical results show same trends and good agreement for the heat transfer and nearly identical values for pressure drop.

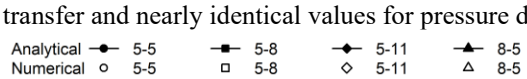

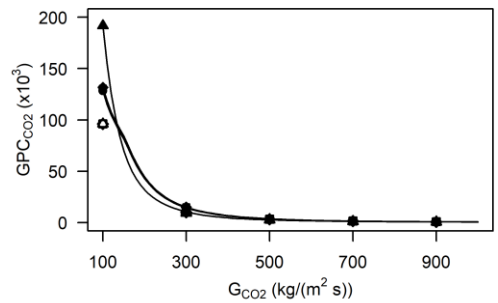

Figure 16: Global performance criterion results of the CO_2 for different channel diameter.

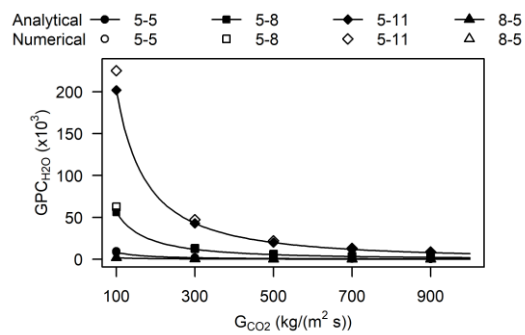

Figure 17: Global performance criterion results of the coolant for different channel diameter.

Based on this optimization an internal fin structure of the channels was investigated. Here different internal fin heights were modeled and numerical simulated by the CFD code. The fin height was varied between 0.04 mm and 0.12 mm and the heat transfer and pressure drop was calculated as before. The fin design and the temperature distribution of both channels is shown in Figure 18 for the different fins.

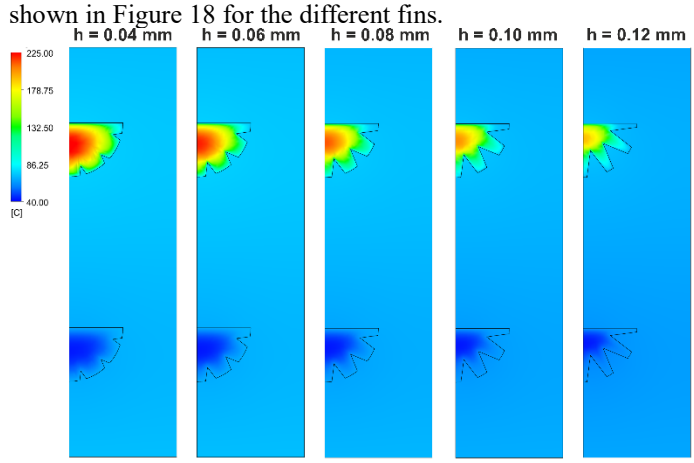

Figure 18: Temperature distribution of both channels for different fin heights.

In Figure 19 the volumetric heat flux and in Figure 20 the pressure drop are shown as a function of the mass flux density for different internal fin heights. As one can see, the heat transfer increases as the fin height increases, since the turbulence increases and the heat conduction of the fins allow higher

temperatures in the bulk flow of the sCO_2 channel. Nevertheless, the pressure drop along the flow channel rises as the fin height increases. Reason for that is the additional friction surface due to the fins. Similar to the channel diameter a tradeoff between heat transfer and pressure drop needs to be found.

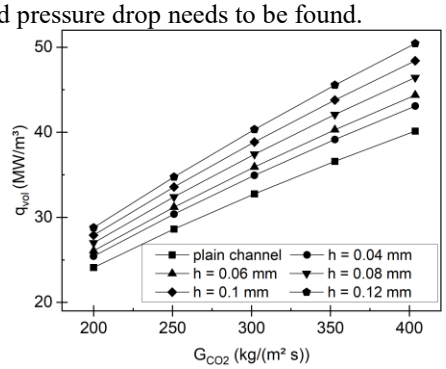

Figure 19: Numerical results of heat transfer and pressure drop for different internal fins in the channel.

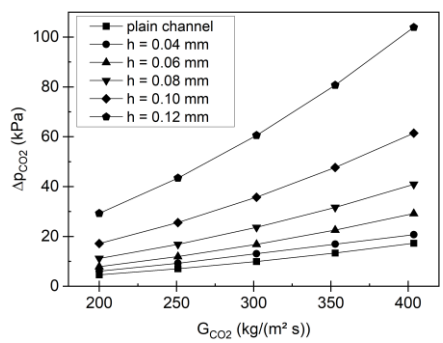

Figure 20: Numerical results of heat transfer and pressure drop for different internal fins in the channel.

In order to determine the optimum fin configuration the ratio of heat transfer to pressure drop will be evaluated by the global performance criterion. In Figure 21 the global performance is shown for different mass fluxes and fin heights. It can be seen, that the fin height of 0.4 mm achieves the greatest global performance followed by the 0.6 mm fins. For fin heights greater than 0.6 mm the higher pressure drop is dominating over the heat transfer enhancement. Hence, the global performance is lower compared to the plain channel. Therefore, a finned channel applying 0.4 mm is recommended for the pre-cooler.

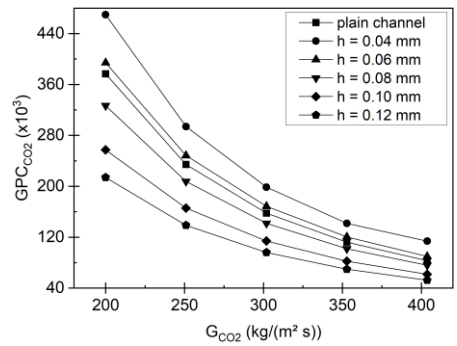

Figure 21: Global performance criterion calculated from the numerical results for different internal fins in the channel.

CONCLUSION

In the present investigation, the design of a pre-cooler for a waste heat driven sCO_2 power cycle was analyzed. Thus, the potential of waste heat recovery were studied and categorized depending on the quantity and the quality of available heat sources. As a reference case, the exhaust gas stream of a turbine of a gas compressor station was used. For this waste heat source, a simple power cycle layout was calculated and the boundary conditions, such as temperature, pressure and mass flow rate, of the liquid cooler were determined. On this base the pre-cooler was calculated analytical by applying heat transfer and pressure drop correlations, and numerical by using the commercial fluid dynamic code ANSYS CFX. Different channel diameters were investigated to determine the optimum heat exchanger design. It was found, that the heat transfer and pressure drop increases for smaller channel diameter, for constant inlet velocity, temperature and pressure. However, the influence of the sCO_2 channel diameter on the pressure drop was small. The global performance criterion was used to determine the optimum design for both channel diameter considering both heat transfer and pressure drop. For the optimum configuration of 0.5 mm sCO_2 channel diameter and 0.8 mm coolant channel diameter an internal fin structure was introduced and the fin height was analyzed. The heat transfer and the pressure drop increase with fin height. In order to determine the best tradeoff between heat transfer and pressure drop, the global performance was used. Thus, the greatest performance was found for a fin height of 0.4 mm, which can be recommended for the design of a pre-cooler.

NOMENCLATURE

G_{CO2}	mass flux of the CO_2 channel, kg/(m²s)
G_{H2O}	mass flux of the CO_2 channel, kg/(m²s)
GPC_{CO2}	global performance criteria of the CO_2 channel, -
GPC_{H2O}	global performance criteria of the coolant channel, -
h	internal fin height, m
$\dot{m}_{CO2}$	mass flow rate of the CO_2 stream, kg/s
$\dot{m}_{H2O}$	mass flow rate of the coolant stream, kg/s
$\dot{m}_{wh}$	mass flow rate of the waste heat stream, kg/s
p	pressure, Pa

P_{net}	net power output, W
Δp	pressure difference, Pa
$\dot{Q}_{Heater}$	heat flow rate to the primary heat exchanger, W
$\dot{Q}_{wh}$	heat flow rate of the waste heat stream, W
$\dot{q}_{vol}$	volumetric heat flux density, W/m³
T_b	temperature of the bulk fluid, °C
T_{wh}	temperature of the waste heat stream, °C
U	overall heat transfer coefficient, W/m²K
z_{pos}	longitudinal positions along the channel, m
α	heat transfer coefficient, W/mK

ACKNOWLEDGEMENTS

This work is part of the research project CARBOSOLA funded by the German Federal Ministry of Economic Affairs and Energy (BMWi) under the grant number 03EE5001D. Responsibility if the content of this publication lies with the authors.

REFERENCES

[1] Federal Ministry for Environment, Nature Conservation and Nuclear Safety, (2016). Klimaschutzplan 2050, pp. 1-96.

[2] Brun K., Friedman P., Dennis R. (2017). Fundamentals and Applications of Supercritical Carbon Dioxide (sCO2) Based Power Cycles. ISBN: 978-0081008041.

[3] Liao S. M., Zhao T. S. (2002). Measurements of Heat Transfer Coefficients from Supercritical Carbon Dioxide Flowing in Horizontal Mini/Micro Channels. Journal of Heat Transfer 124, pp. 413-420.

[4] Dang C., Hihara E. (2004). In-tube cooling heat transfer of supercritical carbon dioxide. Part 1. Experimental measurement. International Journal of Refrigeration 27, pp. 736-747.

[5] Ngo T. L., Kato Y., Nikitin K., Ishizuka T. (2007). Heat transfer and pressure drop correlations of microchannel heat exchangers with S-shaped and zigzag. Experimental Thermal and Fluid Science 32, pp. 560-570.

[6] Li H., Kruizenga A., Anderson M., Corradini M., Luo Y., Wang H., Li H. (2011). Development of a new forced convection heat transfer correlation for CO2 in both heating and cooling modes at supercritical pressures. International Journal of Thermal Sciences 50, pp. 2430-2442.

[7] Pitla P. P., Groll E. A., Ramadhyani S. (2002). New correlation to predict the heat transfer coefficient during in-tube cooling of turbulent supercritical CO2. International Journal of Refrigeration 25, pp. 887-895.

[8] Van Abel E. N., Anderson M. H., Corradini M. L. (2011). Numerical investigation of pressure drop and local heat transfer of supercritical CO2 in printed circuit heat exchangers. Supercritical CO2 Power Cycle Symposium. Boulder, USA.

[9] Serrano I. P., Cantizano A., Linares J. I., Moratilla B. Y. (2014). Modeling and sizing of the heat exchangers of a new supercritical CO2 Brayton power cycle for energy conversion for fusion reactors. Fusion Engineering and Design 89, pp. 1905-1908.

[10] Xu X., Ma T., Li L., Zeng M., Chen Y., Huang Y., Wang Q. (2014). Optimization of fin arrangement and channel configuration in an airfoil fin PCHE for supercritical CO2 cycle. Applied Thermal Engineering 70, pp. 867-875.

[11] Baik J.-Y., Jeon S., Kim B., Jeon D., Byon C. (2017). Heat transfer performance of wavy-channeled PCHEs and the effects of waviness factors. International Journal of Heat and Mass Transfer 114, pp. 809-815.

[12] Wang J., Guan Z., Gurgenci H., Veeraragavan A., Kang X., Hooman K. (2019). A computationally derived heat transfer correlation for in-tube cooling turbulent supercritical CO2. International Journal of Thermal Sciences 138, pp. 190-205.

[13] Heat Roadmap Europe. URL: https://heatroadmap.eu/.

[14] Connolly D. (2013). Heat Roadmap Europe 2050. Second pre-study for the EU27. Tech. rep.. Aalborg University, Halmstad University, Ecofys Germany GmbH, PlanEnergi.

[15] Persson U., Möller B., Werner S. (2014). Heat Roadmap Europe: Identifying strategic heat synergy regions. Energy Policy 74, pp. 663-681.

[16] Brückner S. (2016), Industrielle Abwärme in Deutschland - Bestimmung von gesichertem Aufkommen und technischer bzw. wirtschaftlicher Nutzbarkeit. PhD Thesis, TU Munich.

[17] MAN Diesel & Turbo. THM Gas Turbines. URL: https://turbomachinery.mandieselturbo.com/docs/librariesprovider4/Turbomachinery_doc/thm-gas-turbines.pdf?sfvrsn=14.

[18] Yuan, Z. (2000). Numerical study of periodically turbulent flow and heat transfer in a channel with transverse fin arrays. International Journal of Numerical Methods for Heat and Fluid Flow 10, pp. 842-861.

[19] Kruizenga A., Anderson M., Fatima R., Corradini M., Towne A., Ranjan D. (2011). Heat Transfer of Supercritical Carbon Dioxide in Printed Circuit Heat Exchanger Geometries. Journal of Thermal Science and Engineering Applications 3.

[20] Jackson J.D. (2002). Consideration of the heat transfer properties of supercritical pressure water in connection with the cooling of advanced nuclear reactors. The 13th pacific basin nuclear conference. Shenzhen, China.

Published in: 4th European sCO2 Conference for Energy Systems, 2021

DOI: 10.17185/duepublico/73968
URN: urn:nbn:de:hbz:464-20210330-112909-8